Kinematic Patterns Associated with the Vertical Force Produced during the Eggbeater Kick

OLIVEIRA, Nuno, CHIU, Chuang-Yuan and SANDERS, Ross

Published version

OLIVEIRA, Nuno, CHIU, Chuang-Yuan and SANDERS, Ross (2015). Kinematic Patterns Associated with the Vertical Force Produced during the Eggbeater Kick. Journal of Sports Sciences, 33 (16), 1675-1681.

Title: Kinematic Patterns Associated with the Vertical Force Produced during the Eggbeater Kick

Running Title: Vertical Force and the Eggbeater Kick

Authors

Nuno Oliveira (1), Chuang-Yuan Chiu (1), Ross H. Sanders (2)

1 - Centre for Aquatics Research and Education, ISPEHS, The University of Edinburgh, United Kingdom

2 - Exercise and Sport Science, FHS, The University of Sydney, Australia

Corresponding Author
Nuno Oliveira
72 Seaman Ave. apt 5D
New York, NY 10034
Phone: +14842011623
Email: nunocancela@gmail.com

Chuang-Yuan Chiu
St Leonard's Land 2.23
Holyrood Rd
Edinburgh, EH8 8AQ, UK
Phone: (+44)01316514109
Email: Thorsten.chiu@gmail.com

Prof. Ross H Sanders
The University of Sydney
C43K - K Block Cumberland Campus
Lidcombe NSW 2141
Australia
Phone: (+61)29351 9067
Email: ross.sanders@sydney.edu.au

Keywords: Biomechanics, Water Polo, Eggbeater Kick, Vertical Force, Joint Angles

Abstract

The purpose of this study was to determine the kinematic patterns that maximized the vertical force produced during the water polo eggbeater kick. Twelve water polo players were tested executing the eggbeater kick with the trunk aligned vertically and with the upper limbs above water while trying to maintain as high a position as possible out of the water for nine eggbeater kick cycles. Lower limb joint angular kinematics, pitch angles and speed of the feet were calculated. The vertical force produced during the eggbeater kick cycle was calculated using inverse dynamics for the independent lower body segments and combined upper body segments, and a participant-specific second degree regression equation for the weight and buoyancy contributions. Vertical force normalized to body weight was associated with hip flexion (Average, $r=0.691$; Maximum, $r=0.791$; Range of Motion, $r=0.710$), hip abduction (Maximum, $r=0.654$), knee flexion (Average, $r=0.716$; Minimum, $r=0.653$) and knee flexion-extension angular velocity ($r=0.758$). Effective orientation of the hips resulted in fast horizontal motion of the feet with positive pitch angles. Vertical motion of the feet was negatively associated with vertical force. A multiple regression model comprising the non-collinear variables of maximum hip abduction, hip flexion range of motion and knee flexion angular velocity accounted for 81% of the variance in normalized vertical force. For high performance in the water polo eggbeater kick players should execute fast horizontal motion with the feet by having large abduction and flexion of the hips, and fast extension and flexion of the knees.

Word Count: 2900

Introduction

The eggbeater kick is a complex and unusual movement typically executed in water polo and synchronized swimming, with the main objective being to elevate the upper body above the water. Elevating the body assists in the performance of skills that involve the use of the upper limbs above water. The lower limb muscles are involved in producing alternating cyclical movements with the lower segments (Oliveira et al., 2010; Klauck et al., 2006) that results in the ability to generate constant propulsive forces on the body that effect the height attained during the eggbeater kick (Dopsaj, 2010; Klauck et al., 2006). Therefore, the height achieved depends on the interaction of variables controlled by the player (Sanders, 1999a). In keeping with the Gibsonian concept of affordances (Gibson, 1976; Greeno, 1994) raising the body affords increased freedom for shooting, passing, and blocking. That is, the upper body and upper limbs are clear of the water enabling increased range of joint motion by reducing the effect of constraints in the form of water resistance. Moreover, height has been used as an indicator of performance and recognized as an important factor in the efficiency of other water polo skills (i.e. shooting, passing, goalkeeper actions) (Davis & Blanksby, 1977; Smith, 1998). However, to further improve understanding of the relationship between technique and performance, analysis of kinetics and kinematics needs to be conducted taking into account the mass of the players.

There have been only a small number of detailed studies on the lower limb kinematics during the eggbeater kick (Sanders, 1999a; Sanders, 1999b; Homma & Homma, 2005). Sanders (1999b) focused on the role of the feet, relating specific variables in the execution of the eggbeater kick (foot velocity, pitch and sweepback angles of the feet, and foot paths) with the height attained. Homma & Homma (2005) proposed coaching guidelines for the technique of the eggbeater kick by investigating kinematic parameters of the lower limbs between synchronized swimmers of different levels of performance (excellent-poor). Both studies provided important information about the kinematics of the movement but further detail is needed about the actions of the individual joints involved in the eggbeater kick technique and the vertical force produced over the period of the cycle. Addressing individual joint actions can clarify the role of each joint in the movement and identify more precisely which specific actions are associated with performance. It may be that the variance in performance can be explained by a limited number of kinematic variables.

The purpose of this study was to determine the kinematic patterns that maximize the vertical force produced during the water polo eggbeater kick.

Methods

Participants

Twelve British League Division I male water polo players (aged: 22.41 ± 1.50 years; body mass: 81.25 ± 6.08 kg; height: 184.75 ± 5.11 cm) were tested. At the time of this study, the participants had 4–5 water polo training sessions per week equivalent to approximately 10h per week. Written informed consent was obtained from the participants. All testing procedures were approved by the University of Edinburgh Ethics Committee.

Protocol

Each player was asked to execute the eggbeater kick with the trunk aligned vertically and with the arms elevated above the water while trying to maintain as high a position as possible for the duration of nine cycles.

Five portable ELMO PTC-450C cameras (4 cameras below and 1 above the water surface) recorded the movement. Underwater cameras were attached to the swimming pool wall at different heights and placed 5m away from the subject. The above water camera was placed 7m away from the subject with its axis horizontal. Camera sampling frequency was set at 25 frames per second, with an electronic shutter speed of 1/250 seconds, to reduce the blurring of the image that occurs when recording fast underwater movements. Calibration set-up was similar to Psycharakis et al. (2005). However, a smaller calibrated volume (1.5m x 1.5m x 1m) and closer camera positions were used. This should result in higher accuracy and reliability than that achieved by Psycharakis et al. (2005).

Data Processing

The first nine eggbeater kick cycles of the trial were analyzed. The cycle was defined as the period between two consecutive maximum extensions of the dominant knee. Data were filtered with a 2nd order Butterworth filter with a 6Hz cut-off frequency and interpolated to a 1600Hz frequency signal using a cubic spline function.

Two types of markers placed on specific body landmarks enabled identification of body segments for digitization and calculation of variables while minimizing the drag during the movement of the segments in the water. Participants were marked on both lower limbs with red and black plastic spherical markers (2cm diameter) (middle point between iliac crest and lateral knee marker, middle point between lateral knee and lateral malleolus marker, medial malleolus – tibia, lateral malleolus - fibula, 1st Interphalangeal, 5th Metatarsophalangeal) and black wax skin markers applied with a 4cm diameter sponge (Iliac crest, greater trochanter, medial and lateral epicondyle of the femur, tuberosity of the calcaneus bone). Additionally a black tape (5cm x 1.9cm) on a white tape background was placed in the superior part of the sternum (manubrium) to digitize the above water point. This orientation enabled continuous scaling in the vertical direction so that height could be determined accurately as a function of time.

Four coordinate frames were created in four different segments of the lower limb: pelvis, thigh, shank and foot (Fig. 1). The moving coordinate frame at the pelvis was formed by the hip (left-right) vector (x1), the iliac crest-hip vector (z1), and the cross-product vector of x1 and z1 (y1). The moving coordinate frame for the thigh was formed by the hip-knee vector (z2), cross-product vector of middle femur-hip and middle femur-knee vectors (y2), and the cross-product vector of z2 and y2 (x2). The moving coordinate frame for the shank was formed by the knee-ankle vector (z3), the cross-product vector of middle shank-knee and middle shank-ankle vectors (y3), and the cross-product vector of z3 and y3 (x3). The moving coordinate frame for the foot was formed by the 1^{st} interphalangeal-heel vector (y4); the cross-product vector of the 1^{st} interphalangeal-heel vector and the 5^{th} metatarsophalangeal-heel vector (z4); the cross-product vector of y4 and z4 (x4).

*******Figure 1*******

The sequence of rotation for the hip was flexion/extension (T1) followed by abduction/adduction (T2) then internal/external rotation (T3). The ankle followed the same sequence but different terminology was adopted: plantarflexion/dorsiflexion (T1), inversion/evertion (T2) and adduction/abduction (T3). Following this sequence the resulting transformation matrix (T) was calculated:

$$T = T3 \times T2 \times T1$$

$$T = \begin{bmatrix} cos2 \times cos3 & cos3 \times sin1 \times sin2 - cos1 \times sin3 & sin1 \times sin3 + cos1 \times cos3 \times sin2 \\ cos2 \times sin3 & sin1 \times sin2 \times sin3 + cos1 \times cos3 & cos1 \times sin2 \times sin3 - cos3 \times sin1 \\ -sin2 & cos2 \times sin1 & cos1 \times cos2 \end{bmatrix}$$

From this rotation matrix a solution θ1 (flex/ext), θ2 (abd/add) and θ3 (int/ext rot) for the hip joint, θ1 (flex/ext) for the knee joint, and θ1 (plantarflex/dorsiflex), θ2 (inversion/eversion) and θ3 (adduction/abduction) for the ankle joint was calculated:

$$\theta 2 = -sin^{-1}(T(3,1))$$

$$\theta 1 = cos^{-1}(T(3,3)/\cos(\theta 2))$$

$$\theta 3 = sin^{-1}(T(2,1)/\cos(\theta 2))$$

Angular velocities were calculated using the coordinate frames of each body segment. The angular velocity vector ω = (ω_x, ω_y, ω_z) was extracted from the skew-symmetric matrix S = S(ω):

$$S_{(\omega)} = \begin{bmatrix} 0 & -\omega_z & \omega_y \\ \omega_z & 0 & -\omega_x \\ -\omega_y & \omega_x & 0 \end{bmatrix}$$

Where ω is the angular velocity of the rotating frame with respect to the fixed frame

$S_{(\omega)}$ is the differential of the rotation matrix as follows:

$$S_{(\omega)} = \frac{dR_t}{dt} R_{(t)}^{-1}$$

Where R is the rotation matrix and t is the time interval between frames.

Vertical Force Protocol

The elliptical zone method (Ezone) (Jensen, 1976; Deffeyes & Sanders, 2005) was used to calculate each body segment mass and centre of mass location. Coefficients of variation (from 55 trials) for segment mass ranged from 0.951% (thorax plus abdomen) to 11.90% (neck); coefficients of variation for centre of mass position as a percentage distance between the landmarks ranged from 0.662% (abdomen) to 4.689% (left foot). Landmarks additional to those listed above were used for the Ezone method. These additional landmarks included mandible angle, 2nd cervical vertebra, 7th cervical vertebra, axes of the head of each humerus, acromioclavicular joint, xiphoid process, olecranon process of the ulna, wrist axis, 3rd distal phalanx, greater tubercle of the humerus and vertex of the head.

The vertical force produced during the eggbeater kick was calculated using the following formula:

$$V\ Force_i = ((Weight + buoyancy)_i \times 9.8) + (y\ddot{FSTcom}_i \times FSTmass) + (y\ddot{HAT}_i \times HATmass)$$

i = sample number

To calculate the weight plus buoyancy each participant was suspended in the vertical position using a swimming pool hoist and a harness, these were attached through a load cell that indicated the weight (KgF). Each participant was lowered very slowly until the black tape was no longer visible. This produced a video file where the height (distance from the black tape to water surface) and the corresponding weight plus buoyancy (displayed in the load cell display x 9.8m/s^2) could be determined in each frame and a 2nd degree regression equation calculated. The weight plus buoyancy was calculated by determining the height at each sample during the trial and inserting it into the 2nd degree regression equation previously calculated specifically for each player.

The FST system comprised the feet, shanks and thighs. The mass of the whole system was calculated by adding the segment masses obtained from Ezone. Each coordinate of the system's centre of mass was determined by summing the segmental mass-moments and dividing by the mass of the whole system:

$$Xcom_{fst} = \frac{Xrthigh + Xrshank + Xrfoot + Xlthigh + Xlshank + Xlfoot}{FST\ mass}$$

$$X\ segment = (x1 + ((x2 - x1) \times cmfd)) \times segment\ mass$$

Where x1 is the x coordinate of the proximal marker of the segment, x2 is the distal marker of the segment and *cmfd* is the centre of mass fractional distance calculated with the Ezone method.

The same process was conducted to calculate $Ycom_{fst}$ and $Zcom_{fst}$ for the n samples of each eggbeater kick cyle. Having calculated the coordinates of the feet, shanks and thighs system centre of mass, the vertical acceleration of the system was calculated using the central difference method:

$$y\ddot{FST}com_i = (Ycom_{i+1} - 2(Ycom_i) + Ycom_{i-1}) \times sf^2$$

i = sample number

sf = sample frequency

The head, arms and trunk (HAT) was considered as a one point mass since players were instructed to keep their arms and head completely still, resulting in very limited segmental motion. The head, arms and trunk was represented by the point digitised at the top of the black tape. Thus, the vertical acceleration of the system was calculated as:

$$y\ddot{H}AT_i = (yHAT_{i+1} - 2(yHAT_i) + yHAT_{i-1}) \times sf^2$$

i = sample number

sf = sample frequency

Foot Pitch Angles and Foot Speed

Foot pitch angles, speed and percent contributions of anterior-posterior, medial-lateral and vertical motions of the feet were calculated in MATLAB following the methods outlined by Sanders (1999b). Pitch (θ) is the angle between the plane of the foot and the direction of water flow (Fig. 2):

$$\theta = \left(\frac{\pi}{2} - \cos^{-1}\left[N \cdot \frac{v}{|N||v|}\right]\right) \cdot \frac{360}{2\pi}$$

(v) is the foot velocity vector and N was the vector normal to the plane of the foot determined as the cross-product of the vectors joining the heel marker to each of the phalangeal joint markers. Pitch angle (ranging from -90° to 90°) was positive when water flow hit the plantar surface of the foot and negative when the water flow hit the dorsal surface of the foot.

*****Figure 2******

To calculate the speed of the foot, the centre of the foot was determined as the mean of the three foot markers used (1st interphalangeal joint, 5th metatarsophalangeal joint and heel). X, Y, and Z component velocities were obtained by differentiation with respect to time of the respective foot centre coordinates. The score for foot speed over an *n* samples cycle was:

$$\text{Foot speed score} = \left(\sum_{i=1}^{n} |R_i|^2\right)/n$$

Where R_i is the resultant foot velocity for the n^{th} sample.

As calculated by Sanders (1999b), the percentage of velocity components was the sum, across the cycle, of the squared instantaneous velocity components expressed as a percentage of the sum of the squares of the foot speed.

Statistical Analysis

For each variable the score of each subject was the mean across the nine cycles of the intra-cycle average, maximum or minimum value for both sides. The Pearson product-moment correlation coefficient (*r*) was calculated using SPSS (version 20.0.0) to measure the linear correlation (dependence) between kinematic variables and performance (vertical force normalized to body weight). All correlations were tested for an alpha level of 0.05. The coefficients for the vertical force model were calculated using the regression analysis function in Excel 2010 (version 14.0).

Results

Joint Angles

Table 1 shows the scores across all subjects for the joint angles calculated.

*******Table 1*********

Table 2 shows the correlation coefficients between vertical force normalized to body weight and the joint angles calculated. Correlations were significant ($p<0.05$) for maximum hip abduction and hip abduction range of motion; average, maximum, and minimum hip flexion; average and minimum knee flexion, and knee flexion/extension average angular velocity.

********Table 2*********

Foot Motion

Table 3 shows the scores across all participants for foot speed, foot pitch angles and foot motion and the correlation coefficients between vertical force normalized to body weight and the foot speed, foot pitch angles and foot motion. A significant negative correlation ($p<0.05$) was observed for vertical foot motion.

*********Table 3*********

Discussion

Kinematic Factors Affecting Eggbeater Kick Performance

The average vertical force normalized to body weight was the performance indicator in this study. Thus better players were considered to produce greater vertical force normalized to body weight during the eggbeater kick cycle. The results revealed which aspects of the eggbeater kick motion are associated with high level performance and help distinguish players in terms of ability. Based on correlations between kinematic parameters and the vertical force normalized to body weight it is apparent that better players were characterized by large maximum abduction (r=0.654, p=0.021) and average flexion (r=0.691, p=0.013) of the hips throughout the cycle. Although Homma & Homma (2005) investigated the eggbeater kick in synchronized swimmers, this author highlighted similar features in excellent eggbeater kick performers: knees were held as high and near the water surface, heels were kept close to the hips and knees were kept as wide as possible. Average knee flexion was also correlated with performance (*r*=0.716, *p*=0.009) giving an advantage to players that keep their knees more flexed during the cycle. However, average knee flexion positively correlated with performance due to lower maximum knee extension (*r*=0.653, *p*=0.021) rather than larger maximum knee flexion values (*r*=0.085, *p*=0.794). This result agrees with Sanders (1999b) who noted that excessive extension would be a disadvantage because of the difficulty of recovering the foot without having substantial magnitude and duration of negative pitch.

The direction of motion of the feet is also an important factor in eggbeater kicking since vertical motion of the feet was negatively correlated with performance (*r*=-0.590, *p*=0.043). Additionally, the duration of positive pitch angles in the feet was correlated with anterior-posterior motion (*r*=0.731, *p*=0.007) and negatively correlated with vertical motion (*r*=-0.743, *p*=0.006). It is clear that the hips control the motion of the feet, maximum abduction (*r*=0.494, *p*=0.102) and flexion (*r*=0.468, *p*=0.125) of the hip were correlated with anterior-posterior motion and medio-lateral motion of the feet respectively. Moreover, both maximum hip abduction and flexion were negatively correlated with vertical motion of the feet (abduction: *r*=-0.415, *p*=0.180; flexion: *r*=-0.545, *p*=0.067). Sanders (1999b) reported that vertical and anterior-posterior components of foot velocity (*r*=-0.72 and *r*=0.72, respectively) were strongly related to height, suggesting that horizontal motion of the feet during the cycle is more favourable than vertical motion for height attained. Horizontal motion creates longer periods of positive pitch angles whereas the upwards motion of the feet creates negative pitch angles and forces tending to push the player downwards.

Vertical Force Model

The average vertical force normalized to body weight produced during the cycle ranged from 2.07 N/Kg to 3.12 N/Kg. Multiple regression analysis yielded a model that accounted for 81% (adjusted R squared) of the variance in vertical force:

$$Vertical\ Force = 0.6372 + 0.0135 \times \max hip\ abduction + 0.0124 \times hip\ flexion\ ROM + 0.0031 \times average\ knee\ flexion\ angular\ velocity$$

The three variables have low degrees of collinearity as indicated by the correlations between them: maximum hip abduction and hip flexion range of motion (r=0.244); maximum hip abduction and average knee flexion angular velocity (r=0.381); hip flexion range of motion and average knee flexion angular velocity (r=0.487). Thus, the variance explained by the model was close to the sum of the variance explained by the individual variables (86%).

The variables used in this model cover the body position and orientation of the lower limbs (maximum hip abduction and hip flexion range of motion) during the movement and the speed of the motion (average knee flexion angular velocity).

Maximum hip abduction was correlated with vertical force (*r*=0.654, *p*=0.021). It contributed to maintaining positive pitch angles (*r*=0.627, *p*=0.029) for longer duration (*r*=0.539, *p*=0.071) as well as being related to the horizontal motion of the feet.

The hip flexion-extension range of motion was correlated with the vertical force (*r*=0.710, *p*=0.010). Because both maximum (*r*=0.791, *p*=0.002) and minimum (*r*=0.612, *p*=0.034) hip flexion were correlated with performance, a large hip flexion-extension range of motion should be maintained. Hip flexion-extension range of motion contributed to the medial-lateral motion of the feet (*r*=0.605, *p*=0.037) and was negatively correlated with the vertical motion (*r*=-0.520, *p*=0.083). Additionally it contributed to foot speed during the cycle (*r*=0.646, *p*=0.023).

The average knee flexion-extension angular velocity included the phase of flexion and extension of the knee. Its main role in the cycle was to move the feet quickly, hence its correlation with foot speed (*r*=0.583, *p*=0.047). Additionally, players that exhibited large knee angular velocities had small vertical foot motion (*r*=-0.688, *p*=0.013).

Conclusion

Performance of the water polo eggbeater kick is optimised by a limited group of kinematic parameters. Large average hip flexion range of motion and maximum hip abduction together with fast knee flexion and extension are associated with performance. A vertical force model containing these three variables explained 81% of vertical force variance.

References

Davis, T. & Blanksby, B. A. (1977). A cinematographic analysis of the overhand water polo throw. *Journal Sports Medicine Physical Fitness*, 17**,** 5-16. Retrieved from http://www.ncbi.nlm.nih.gov/pubmed/895115

Deffeyes, J. & Sanders, R.H. (2005). Elliptical zone body segment modeling software: Digitising, modeling and body segment parameter calculation. In: Q. Wang (ed.) *Proceedings of XXIII International Symposium on Biomechanics in Sports*. The China Institute of Sports Science, Beijing, pp. 749-752. Retrieved from https://ojs.ub.uni-konstanz.de/cpa/article/download/1174/1061

Dopsaj, M. (2010). Pulling Force Characteristics of 10 s Maximal Tethered Eggbeater Kick in Elite Water Polo Players: A Pilot Study. *XIth International Symposium for Biomechanics & Medicine in Swim*, 11, 69. Retrieved from http://www.abraldes.org/Documentos/00745-chapter.pdf

Gibson, J.J. (1979). *The Ecological Approach to Visual Perception*. Houghton Mifflin, Boston, MA.

Greeno, J.G. (1994). Gibson's Affordances. *Psychological Review*, 101, 336-342. DOI: 10.1037/0033-295X.101.2.336

Homma, M. & Homma, M. (2005). Coaching points for the technique of the eggbeater kick in synchronized swimming based on three-dimensional motion analysis. *Sports Biomechanics*, 4, 73-87. DOI: 10.1080/14763140508522853

Jensen, R. K. (1976). Model for body segment parameters. In: Komi, P. V. (ed.), *Biomechanics V-B*. Baltimore, MD: University Park Press.

Klauck, J., Daniel, K. & Bayat, M. (2006). Goalkeeper's eggbeater kick in water polo: kinematics, dynamics and muscular coordination. In: *Biomechanics and Medicine in Swimming X*, 56-58. Retrieved from http://www.fade.up.pt/rpcd/_arquivo/RPCD_vol.6_supl.2.pdf

Oliveira, N., Fernandes, R. J., Sarmento, M., Liberal, S., Figueiredo, P. A., Gonçalves, P. & Villas-Boas, J. P. (2010). Muscle Activity During the Typical Water Polo Eggbeater Kick. *International Journal of Aquatic Research & Education,* 4**,** 163-174. Retrieved from http://journals.humankinetics.com/ijare-back-issues/ijarevolume4issue2may/muscle-activity-during-the-typical-water-polo-eggbeater-kick

Psycharakis, S. G., Sanders, R. H. & Mill, F. (2005). A calibration frame for 3D analysis of swimming. In: *XXIII International Symposium on Biomechanics in Sports*. The China Institute of Sports Science, Beijing. Retrieved from https://ojs.ub.uni-konstanz.de/cpa/article/view/1134/1023

Sanders, R. H. (1999a). Analysis of the eggbeater kick used to maintain height in water polo. *Journal of Applied Biomechanics*, 15, 284-291. Retrieved from http://journals.humankinetics.com/jab-back-issues/JABVolume15Issue3August/AnalysisoftheEggbeaterKickUsedtoMaintainHeightinWaterPolo

Sanders, R. H. (1999b). A model of kinematic variables determining height achieved in water polo boosts. *Journal of Applied Biomechanics*, 15, 270-283. Retrieved from http://journals.humankinetics.com/jab-back-issues/JABVolume15Issue3August/AModelofKinemaicVariablesDeterminingHeightAchievedinWaterPoloBoosts

Smith, H. K. (1998). Applied physiology of water polo. *Sports Medicine*, 26**,** 317-34. **DOI:** 10.2165/00007256-199826050-00003

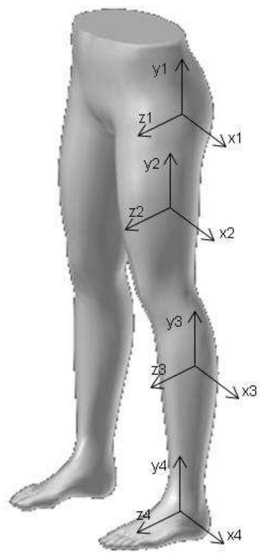

Figure 1. Segments axes of rotation.

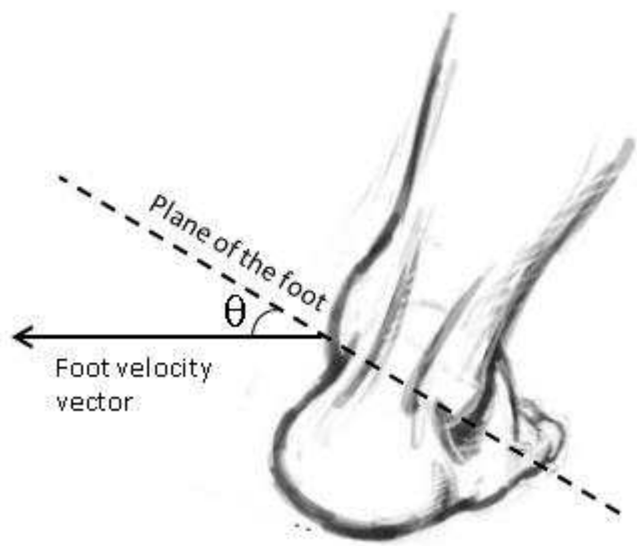

Figure 2. Illustration of foot pitch angle (θ).

Table 1. Mean ± SD of joint variables calculated across all subjects.

	Hip Abduction	Hip Flexion	Hip Internal Rotation	Knee Flexion	Ankle Inversion	Ankle Plantarflexion	Ankle Adduction
Average (°)	34.05 ± 7.24	45.59 ± 10.33	20.35 ± 8.09	91.02 ± 4.92	2.24 ± 3.16	20.75 ± 4.59	20.79 ± 8.58
Maximum (°)	40.83 ± 8.06	64.19 ± 14.11	46.84 ± 8.85	142.38 ± 5.61	25.36 ± 5.83	44.57 ± 3.98	43.79 ± 10.33
Minimum (°)	7.34 ± 7.3	31.29 ± 7.61	-12.16 ± 11.65	37.91 ± 8.82	-9.11 ± 6.72	-18.27 ± 4.74	-4.00 ± 10.82
Range of Motion (°)	33.48 ± 3.32	32.89 ± 9.15	59.01 ± 10.64	104.47 ± 11.26	34.48 ± 4.17	62.85 ± 7.60	48.21 ± 12.16
Average Angular Velocity (°/s)	245.53 ± 46.38	208.92 ± 31.26	229.82 ± 47.66	316.69 ± 35.12	225.80 ± 23.77	263.85 ± 42.58	303.07 ± 53.57

Table 2. Correlation coefficient (*r*), *p* value and r^2 between average vertical force normalized to body weight and joint variables. * indicates statistical significant (p<0.05).

		Hip Abduction	Hip Flexion	Hip Internal Rotation	Knee Flexion	Ankle Inversion	Ankle Plantarflexion	Ankle Adduction
Average	*r*	.562	.691	-.332	.716	-.009	-.001	.286
	p	.057	.013*	.292	.009*	.978	.998	.368
	r^2	.316	.477	.110	.513	.000	.000	.082
Maximum	*r*	.654	.791	-.278	.085	.082	.112	.287
	p	.021*	.002*	.381	.794	.800	.728	.366
	r^2	.428	.626	.078	.007	.007	.013	.082
Minimum	*r*	.455	.612	-.256	.653	.015	-.408	.101
	p	.137	.034*	.422	.021*	.963	.188	.755
	r^2	.207	.375	.066	.426	.000	.166	.010
Range of Motion	*r*	.587	.710	.049	-.469	.091	.314	.225
	p	.045*	.010*	.880	.124	.779	.321	.482
	r^2	.344	.504	.002	.220	.008	.098	.050
Average Angular Velocity	*r*	.141	.540	.361	.758	.173	.465	.216
	p	.663	.070	.250	.004*	.590	.128	.501
	r^2	.020	.291	.130	.575	.030	.216	.047

Table 3. Mean ± SD of foot variables calculated across all subjects, and correlation coefficient (*r*), *p* value and r^2 between average vertical force normalized to body weight and foot variables.

	Foot Speed (m/s)	Foot Pitch Angles (°)			Duration of Positive Pitch (%)	Foot Motion (%)		
		Average	Maximum	Minimum		Anterior-Posterior	Medial-Lateral	Vertical
	2.75 ± 0.11	10.34 ± 3.79	57.27 ± 9.06	-35.74 ± 7.73	64.01 ± 4.30	28.02 ± 4.54	33.09 ± 4.76	37.38 ± 7.18
r	.416	.203	.436	-.244	.282	.108	.330	-0.59
p	.179	.528	.157	.445	.375	.738	.295	.043
r^2	.173	.041	.190	.059	.079	.012	.109	.348